https://doi.org/10.1590/jatm.v18.1409 ORIGINAL PAPER

Robust and Optimal Trajectory Design of a Space Transportation System by Various Heuristic Optimization Methods

Seyyed Ali Saadatdar Arani[1], Mehran Nosratollahi[1*], Yousef Abbasi[1], Amir Hossein Adami[1]

1. Malek-Ashtar University of Technology – Department of Aerospace –Tehran – Iran.

*Corresponding author: mnosratollahi@gmail.com

ABSTRACT

This paper presents a robust optimization framework for Satellite Launch Vehicle (SLV) and upper stage trajectory design, integrating uncertainties to enhance flight performance, minimize steering workload, and improve reliability. Identifying a robust optimal trajectory under uncertainty is crucial. The methodology begins with developing a robust trajectory for a two-stage SLV. The upper stage trajectory was then optimized assuming the first stage remained fixed. Three-dimensional equations of motion served as constraints. Uncertainties (aerodynamic coefficients, dry mass, engine thrust) were modeled via mean and standard deviation. Four metaheuristic algorithms—genetic algorithm (GA), particle swarm optimization (PSO), grey wolf optimizer (GWO), and invasive weed optimization (IWO)—were utilized. Monte Carlo simulations with 300 iterations incorporated uncertainties. Results show significant trajectory accuracy improvements. For the upper stage, altitude error decreased by 77%, orbital velocity error by 68%, and flight path angle error by 90%. For the SLV, altitude error improved by 80%, orbital velocity error by 78%, and flight path angle error by 82%. These findings demonstrate the framework's effectiveness in enhancing trajectory performance under uncertainty.

Keywords: Trajectory optimization, Launch vehicles, Upper stages, Robust design, Metaheuristic algorithms.

INTRODUCTION

A frequent cause of space mission failures is the Satellite Launch Vehicle's (SLV) inability to adhere to its predetermined flight trajectory. This can be attributed to inaccurate forecasting of factors and parameters that impact the system, often stemming from unexpected changes in the environmental or system conditions.

Uncertainty is a crucial factor in many engineering problems because it is often impossible to predict accurately the parameters and factors that affect the outcome. At best, we can only estimate them. Uncertainty refers to the range between complete certainty and pure uncertainty that could impact a product or system's future performance and ability to fulfill its mission. In engineering, uncertainties can significantly impact results, making them a critical parameter to be considered (Wazed *et al.* 2009).

Uncertainty can be caused by errors related to the system itself or its inputs. One of the most critical issues for an aerospace system is the expansion or synergism of uncertainties that can negatively affect the system's output (Yao *et al.* 2011).

In many cases, not paying attention to these uncertain factors can have a heavy cost on the system's performance and lead to disruption or even failure of the system's mission. In the operation process of a system, there are many sources of uncertainty, which can come from the spacecraft system itself or its environment and mission conditions.

Received: Apr. 28, 2025 | **Accepted:** Oct. 20, 2025
Peer Review History: Single Blind Peer Review.
Section editor: Paulo Renato Silva

Therefore, considering the existence of uncertainty in design, one should know and use methods of dealing with uncertainty to reduce its adverse effects on design. One way to be robust against uncertainties is to apply confidence coefficients. So far, there has not yet been a precise and comprehensive method for defining these coefficients. With larger confidence coefficients, design and optimization tend to arrive at solutions that are too conservative, while with smaller confidence coefficients, system reliability cannot be guaranteed. In addition, previous experiences regarding the reliability factor may be inappropriate or outdated for existing structures, thus leading to potential risks. Therefore, the traditional methods of dealing with uncertainties are not adequate enough to improve economically the system's reliability, robustness, and performance. Therefore, this issue has strongly driven the development of design methods based on analytical uncertainty, accuracy, and advancements in mathematical theory, as well as the systematic and rational treatment of uncertainties during design (Padmanabhan 2003).

Among the methods of dealing with uncertainty, the robust approach is an effective method. Much research has been conducted in this regard, and many articles on its theory and application have been published, so it has found its place in many fields, such as aerospace engineering, electricity, industry, civil engineering, management, etc. In the following, to get acquainted with the work done so far, the research done will be reviewed.

Among the first works in uncertainty and robust optimization, we can mention the steps taken by Suister (Zardashti *et al.* 2020). Nevertheless, the presented model has been far from the optimal solution due to excessive caution.

The attempt to optimize a system is to achieve the minimum or maximum of the criterion function or the performance of that system in such a way that the system's efficiency is finally improved. The complexity of aerospace systems is so great that it is impossible to obtain their optimal solution by analytical methods in an acceptable period. Therefore, there is no solution to settle for near-optimal solutions obtained from numerical methods in such a way that they are of acceptable quality and can be obtained in an acceptable timeframe (Wazed *et al.* 2009). In addition, Yao *et al.* (2011) introduced a linear model that achieves a balance between optimization and robustness in solutions. Padmanabhan (2003) presented a multiobjective optimization with a reliability assignment approach. Haimes (1994) introduced a multiobjective optimization model in the presence of uncertainties, and Hattis and Burmaster (1994) presented a model of uncertainties and their analysis. Youn and Wang (2006) also proposed a method for the effect of adding reliability in design in the face of uncertainties. Hosseini *et al.* (2011) examined optimization methods and the multidisciplinary optimal design of an SLV. Zardashti *et al.* (2020) investigated the robust optimal method for the robust trajectory design of a satellite carrier and used the evolutionary optimizer to solve the problem.

Yager *et al.* (1994) have expressed methods for combining multiobjective optimization with robust design. Sentz and Ferson (2002) proposed a formulation and an algorithm to optimize the design in the presence of uncertainty from the point of view of the system's robustness; they presented an independent method to separate design based on robustness from the analysis of nondesign cognitive variables to achieve computational efficiency.

Bataleblu *et al.* (2011) presented a thesis addressing the multiobjective optimization problem with Robust methods to reduce the SLV's mass. Liu and Lu (2013) presented a formulation and algorithm for generating optimal limited Trajectory for meeting in an arbitrary orbit. Paiva *et al.* (2014) offered a comprehensive approach to analyzing, optimizing, and incorporating reliability into aircraft design. The model combines certainty with the simultaneous analysis of reliability and optimization, resulting in a simplified formulation for tackling optimization problems and mitigating predictability.

Okada *et al.* (2015) presented an article in which the design of a robust trajectory in the presence of uncertainties for a projectile is discussed. In order to check the effectiveness of the proposed method, it has been evaluated by Monte Carlo analysis. Shi *et al.* (2023) delved into the subject of optimal robust design methodology and applies it to the optimization of a plane wing. Luo and Yang (2017) discussed uncertainty in orbital parameters; their simulation also uses the Monte Carlo method and linear models.

According to Su and Wang (2015), a trajectory optimization technique employing a robust approach has been proposed for the return phase of a reusable space vehicle. Grant and Bolender (2016) introduced an efficient robust trajectory design methodology using an indirect optimization framework, which integrates worst-case scenarios and robustness considerations to generate solutions that balance performance and robustness. Xue and Duan (2017) presented a research paper about attitude robust control for a reusable spacecraft during the reentry phase. The research methodology utilized fractional calculus and Pigeon-inspired optimization techniques to achieve the desired outcomes. Mirshams *et al.* (2016) presented a combination of multiobjective optimization with

robust optimization to design an SLV with minimum mass and maximum resistance against uncertainties. The Greylag Goose Optimization algorithm, inspired by geese's V-shaped flight, was introduced and validated on University of California, Irvine datasets, benchmark functions, and engineering case studies, showing superior performance in statistical tests (El-Kenawy *et al.* 2024). Selim and Ozkol (2023) presented a robust multidisciplinary method to guide an SLV in the presence of uncertainties for correct closed and open-loop guidance. Also, Roshanian *et al.* (2013) discussed the optimal robust design of an SLV, with the objective of minimizing the total mass of the vehicle while ensuring that all mission and trajectory constraints are met. Additionally, the objective function should be able to withstand operational uncertainties and variations. In Ansaripour *et al.* (2019), the optimal trajectory for a two-stage launch vehicle has been designed to transport a payload to a specific Altitude and velocity. One objective of this reference is to find the optimal pitch program angle as a control variable for the aforementioned problem.

The application of robust optimization and metaheuristic algorithms extends beyond aerospace engineering, demonstrating their effectiveness across various engineering domains. This cross-disciplinary adoption highlights the universality and adaptability of these methodologies in addressing complex optimization problems under uncertainty. In renewable energy systems, the integration of metaheuristic algorithms with machine learning techniques has shown significant promise. A recurrent neural network forecasting model that incorporates a dynamic fitness Al-Biruni Earth radius algorithm was proposed for wind power prediction, addressing uncertainties caused by climate change and varying weather patterns (Karim *et al.* 2023). Similarly, in feature selection problems, the binary arithmetic optimization algorithm was developed to tackle discrete optimization challenges in pattern recognition and data mining (Khodadadi *et al.* 2023). By converting the continuous search space to binary using sigmoid transfer functions and employing a wrapper-based approach with a K-Nearest Neighbors classifier, binary arithmetic optimization algorithm outperformed Dipper Throated Optimization, particle swarm optimization (PSO), genetic algorithm (GA), and Satin Bowerbird Optimizer across 18 University of California, Irvine benchmark datasets. The hybrid binary sine cosine weighted dipper throated optimization algorithm further demonstrated the effectiveness of combining complementary algorithmic strengths (Abdelhamid *et al.* 2023). In electromagnetic antenna design, machine learning ensemble models combined with metaheuristic optimization represent an advanced approach for metamaterial antennas (El-Kenawy *et al.* 2022). The success of these methodologies across renewable energy forecasting, feature selection, and antenna design validates the role of metaheuristic optimization techniques as fundamental tools for addressing complex engineering challenges under uncertainty, paralleling their effectiveness in aerospace trajectory optimization and robust design applications.

In this paper, the optimization problem is first considered by applying the payload mass maximization criterion as a cost function and three-dimensional equations of motion as the constraint equations. Then, the robust optimizer model is constructed by incorporating the mean and standard-deviation parameters of the relevant uncertainties, including the SLV aerodynamic coefficients, dry mass, and engine thrust. In the following, four different metaheuristic optimization methods—the GA, PSO, grey wolf optimizer (GWO), and invasive weed optimization (IWO)—were utilized to optimize the model. Monte Carlo simulation for 300 iterations was used to analyze uncertainties and feed the information back to the optimizer model.

At first, the problem is solved to design a robust optimal trajectory of a two-stage SLV. Then, assuming that the design of the first stage of SLV is already fixed, the design of the trajectory for the upper stage of this SLV proceeds using this method. To achieve this purpose, the remainder of the paper is organized as follows: The next section introduces the mathematical modeling of the SLV, followed by a detailed presentation of the optimization formulation, which is divided into two distinct cases: deterministic optimal and robust optimal formulations; the results of the simulations are discussed in a later section, and the paper concludes with a summary of the key insights and contributions in the final section.

MATHEMATICAL MODELING

Equations of Motion

In general, the equations of motion can be divided into two groups (Zipfel 2007): 1. Kinematic equations, which express the geometric relationship between the movement variables; 2. Dynamic (kinetic) equations, which are extracted using physical laws. The fundamental physical laws related to flight dynamics, Newton's laws of motion and gravity, and aerodynamic principles are based on which forces, aerodynamic moments, and thrusters are calculated.

The dynamic model employs a 3-degrees of freedom translational equations of motion, which describe the behavior of a variable-mass point within the rotating Earth-centered Earth-fixed reference frame. These equations are formulated to represent the translational position vector, denoted as $[h;\ \tau;\ \lambda]T$, and the velocity vector, expressed as $[V;\ \gamma;\ \Psi]T$, both defined in spherical coordinates (Zardashti *et al.* 2020) (Eq. 1):

$$\dot{\tau} = \frac{V\cos\gamma\sin\psi}{r}$$
$$\dot{\lambda} = \frac{V\ \cos\gamma\cos\psi}{r\cos\varphi}$$
$$\dot{h} = V\sin y$$
$$\dot{V} = \frac{1}{m}(T\ \cos\alpha - D - mg\ \sin\gamma) + r\omega^2\cos\varphi(\cos\varphi\sin\gamma - \sin\varphi\cos\gamma\sin\psi) \quad (1)$$
$$\dot{\gamma} = \frac{1}{mV}[(T\sin\alpha + L)\cos\mu - mg\cos\gamma] + \frac{V\cos\gamma}{r} + 2\omega\cos\varphi\cos\psi + \frac{r\omega^2}{V}\cos\varphi(\cos\varphi\cos\gamma + \sin\varphi\sin\gamma\sin\psi)$$
$$\dot{\psi} = -\frac{1}{mV\cos\gamma}(T\sin\alpha + L)\sin\mu - \frac{V}{r}\tan\varphi\cos\gamma\cos\psi + 2\omega(\cos\varphi\tan\gamma\sin\psi - \sin\varphi) - \frac{r\omega^2}{V\cos\gamma}(\cos\varphi\sin\varphi\cos\psi)$$
$$\dot{m} = -\frac{1}{I_{sp}g_0}T_{vac}$$

where l represents longitude, τ denotes latitude, h is the altitude above mean sea level, V is the total velocity, γ is the flight path angle, ψ is the heading angle, m is the mass, r is the radial distance from the Earth's center to the vehicle's center of mass, ω is the Earth's angular velocity, D is the drag force, L is the lift force, T is the thrust, I_{sp} is the specific impulse, α is the angle of attack, and μ is the velocity roll angle (assumed to be zero in this manuscript).

Pitching Program for the SLV Trajectory

The SLV's movement is guided, so a pitch angle is needed as a control function to meet flight requirements (Vinh 1981). These requirements include achieving the correct altitude and velocity for orbit while maintaining a trajectory angle of zero during orbital injection. The method is based on a table of changes of the flight path angle as a function of time, velocity, or altitude that the SLV follows, which is called preset guidance. This table is obtained by solving the flight equations of the SLV and applying the above rule, which is usually obtained in off-line mode. This program is presented in Eq. 2:

$$\theta = \frac{\pi}{2} + \left(\frac{\pi}{2} - \theta_1\right)\left(\bar{t}^2 - 2\bar{t}\right);\quad \bar{t} = \frac{t - t_0}{t_1 - t_0} \quad (2)$$

where t_0 is the duration of the SLV's vertical flight at the beginning of the trajectory, t_1 is the time of the first staging, θ_1 is the value of the pitch angle at this time, and t_f is the burnout (final) time. These three parameters are achieved in the optimization design process.

Furthermore, for the angle of attack program, its equation based on the limitations of the angle of attack, which is affected by the problems of aerodynamic heating and structural loads, is determined in terms of time, as shown in Eq. 3:

$$\alpha(t) = 4\alpha_{max}e^{-a(t-t_0)}\left(e^{-a(t-t_0)} - 1\right) \quad (3)$$

where the α_{max} maximum allowable value of the angle of attack and α is the time constant of the change of the angle of attack, which depends on the type of launcher.

Aerodynamics

Aerodynamic forces exert a significant influence due to the interaction between air particles and the body of the vehicle. Among the critical factors influencing the aerodynamics of the SLV is the structural design of its shape. The forces and moments acting on the vehicle are primarily governed by aerodynamic coefficients, as referenced in Taheri *et al.* (2013). These coefficients determine the magnitude of drag, lift, and momentum forces. Equations 4–6 represent these forces:

$$D = qS_bC_D \tag{4}$$

$$L = qS_bC_L \tag{5}$$

$$M_A = qS_blC_m \tag{6}$$

in which the aerodynamic coefficients of C_D and C_L are obtained with respect to the Mach number and the angle of attack variations, given in Eq. 7 (Ghapanvary *et al.* 2021):

$$C_D = C_D(M,\alpha), C_L = C_L(M,\alpha) \tag{7}$$

Gravity Model

The Earth is modeled as a rotating spherical body, with its surface defined by the mean sea-level radius, denoted as r_0. The gravitational acceleration is assumed to vary with altitude, adhering to the inverse-square law, as detailed by Zheng *et al.* (2020) (Eq. 8):

$$g = g_0(\frac{r_0}{r})^2 \tag{8}$$

here, r_0 represents the mean sea-level radius of the Earth, with a value of 6,371 km, and g_0 denotes the standard gravitational acceleration at the Earth's surface, defined as 9.80665 m·s^{-2}.

Propulsion

The SLV is powered by engines utilizing UDMH/N_2O_4 as the propellant, which are integrated into the main body and distributed across two stages. The first stage operates until its propellant is fully expended, while the upper stage continues to burn until the payload is successfully inserted into its designated orbit, as outlined by Adami *et al.* (2017) (Eqs. 9–10):

$$T' = T'_{vac} - pA'_e \tag{9}$$

$$I_{sp} = I'_{sp} \tag{10}$$

here, A_e denotes the exit area, and the prime symbol (′) indicates parameters corresponding to a single engine.

Calculation of orbital Velocity and inclination angle

Equation 11 is used to calculate the final velocity at the moment of injection in the target orbit (Shaver and Hull 1990):

$$V_i = [V^2 + 2Vr\omega\cos\gamma\cos\psi\cos\tau + (r\omega\cos\tau)^2]^{\frac{1}{2}} \tag{11}$$

In addition, Eq. 12 is used to calculate the target orbit inclination angle:

$$\cos i = \frac{\cos\tau(V\cos\gamma\cos\psi + r\omega\cos\tau)}{[V^2\cos^2\gamma + 2Vr\omega\cos\gamma\cos\psi\cos\tau + (r\omega\cos\tau)^2]^{\frac{1}{2}}} \tag{12}$$

where τ is the latitude.

OPTIMIZATION DESIGN PROBLEM

Genetic Algorithm Optimization

The GA has demonstrated strong effectiveness as an optimization technique for solving nonlinear problems. The process begins with a randomly generated initial population of candidate solutions. Individuals with higher fitness, as determined by the objective function, are then selected for reproduction. New generations are produced through genetic operations such as crossover and mutation, allowing the algorithm to explore the solution space and converge toward optimal solutions. This process is repeated several times until a certain number of generations have been run or until a solution that is considered optimal is reached. The parameters of an individual to be optimized are represented by a structure called chromosome and a binary coding is adopted (Rostami and Toloei 2015).

Particle Swarm Optimization

The PSO is a population-based computational technique designed to solve optimization problems by iteratively improving candidate solutions based on a defined fitness measure. In PSO, a swarm of particles—each representing a potential solution—navigates the search space by updating their positions and velocities according to simple mathematical rules.

The movement of each particle is influenced by its own best-known position and by the globally best-known position identified by the swarm. As particles explore the search space and discover superior positions, both individual and global best values are updated accordingly. This collective behavior enables the swarm to converge toward optimal or near-optimal solutions over successive iterations (Zhao *et al.* 2023).

Grey Wolf Optimization

The GWO is an algorithm that is inspired by the behavior of grey wolves in nature. This algorithm simulates the leadership hierarchy and hunting mechanism of grey wolves by employing four types of grey wolves—alpha, beta, delta, and omega (Mirjalili *et al.* 2014). Additionally, the algorithm implements the three main steps of hunting: searching for prey, encircling prey, and attacking prey (Talouki and Toloei 2025).

Invasive Weed Optimization

The invasive weed metaheuristic algorithm is an optimization algorithm based on population that aims to find the overall best solution of a given function through simulating the compatibility and randomness of a weed colony. This optimization algorithm is inspired by the behavior of weeds in a limited area, struggling for survival for a limited amount of time. Weeds are powerful grasses that grow aggressively and pose a serious threat to crops.

They are highly resilient and adaptable to environmental changes. The algorithm aims to imitate the robustness, adaptability, and randomness of the weed community in nature (Mehrabian and Lucas 2006).

Figure 1 shows a flowchart of the robust optimization trajectory design with four optimization methods mentioned before.

UNCERTAINTY SOURCES

The sources of uncertainty throughout the life cycle, from the moment of its inception to the retirement of the aerospace vehicle, which affect the phase of design to flight, are categorized as follows (Zardashti *et al.* 2020):

- In the mission review phase, uncertainties arise from variability in the needs and requirements of the mission, the progress of science and technology, economic issues, investment priorities, and cultural and political factors.
- During the design phase, simulations are often used to make calculations. However, uncertainties can arise from these calculations. Three main factors contribute to the uncertainty of computational simulations. These factors are model input and output uncertainty, model structure and parameter uncertainty, and model error.
- In the construction phase, uncertainties arise from human and construction errors, etc.
- In the operation phase, uncertainties arise from operational conditions (environment).

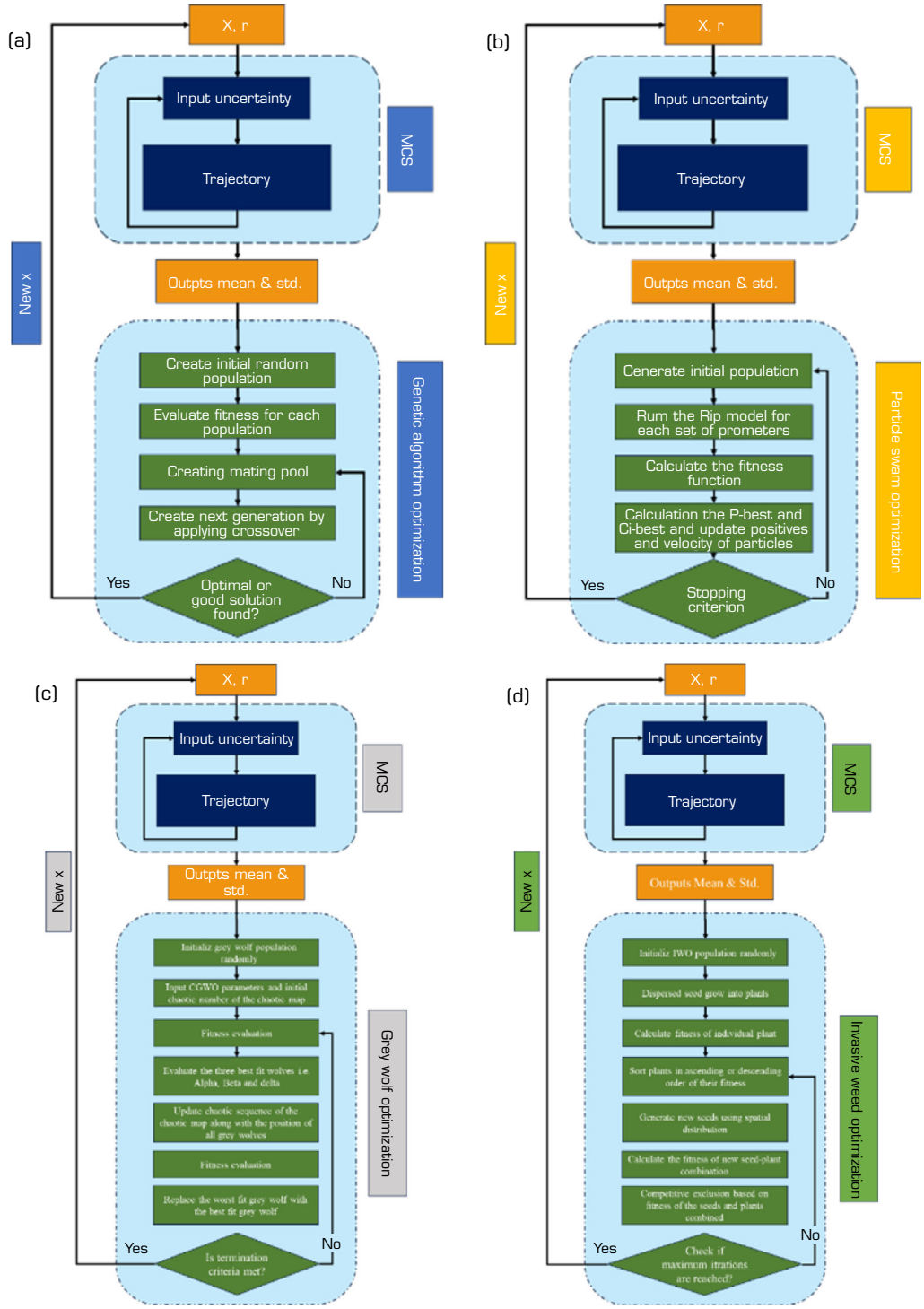

Source: Elaborated by the authors.

Figure 1. Flowchart of the robust optimization trajectory design: a) GA, b) particle swarm (PSO), c) GWO, d) IWO.

Therefore, in this work, some important parameters that have a direct effect on mass and energy characteristics, such as the SLV aerodynamic coefficients, dry mass, and engine thrust, are considered with their appropriate error (disturbed) values as uncertainty sources (Table 1).

Table 1. Error value percentage of parameters.

Parameters		Percentage of error
Aerodynamic	Aerodynamic coefficients	25%
	Atmospheric / environmental (atmospheric density and air pressure)	5%
Engine Thrust		1.5%
Structural	Dry mass	1%
	Manufacturing tolerances	

Source: Elaborated by the authors.

In the following simulation problem, the error is applied as a random process with a normal distribution. The normal distribution function is shown in Eq. 13:

$$f(x;\mu,\sigma^2)=\frac{1}{\sqrt{2\pi\sigma^2}}e^{\frac{-(x-\mu)^2}{(2\sigma^2)}},\qquad x\in R \tag{13}$$

ROBUST OPTIMAL TRAJECTORY FORMULATION IN THE PRESENCE OF UNCERTAINTIES

Robust design seeks to minimize the influence of uncertainties or variations in design parameters on a vehicle's performance, without requiring the complete elimination of these sources of variability (Niazi *et al.* 2024). Therefore, a robust optimal design shows decreased sensitivity to fluctuations in uncontrolled design parameters compared to a deterministic optimal design. A key element of robust design optimization is the formulation of the objective function. This is usually accomplished by calculating the mean and variance (or standard deviation) of the uncertain parameters. Generally, the mathematical framework for robust design optimization can be expressed as shown in Eq. 14:

$$\begin{cases} find & \mathbf{x} \\ \min & \tilde{f}(\mathbf{x})=F(\mathbf{x};\mu_f,\sigma_f) \\ S.t. & \begin{cases} g(\mathbf{x})\le 0 \\ \mathbf{x}^L\le\mathbf{x}\le\mathbf{x}^U \end{cases} \end{cases} \tag{14}$$

here, x represents the design variables, which may include both definite and indefinite parameters, while μ_f and σ_f denote the mean and standard deviation of the uncertain parameters, respectively.

In this study, the mean value of the problem is derived from the final altitude, final velocity, and flight path angle of both the SLV and the upper stage (Eq. 15):

$$\mu_h^f=\frac{1}{n}\sum_i^n h_i^f,\qquad \mu_v^f=\frac{1}{n}\sum_i^n v_i^f,\qquad \mu_\gamma^f=\frac{1}{n}\sum_i^n \gamma_i^f \tag{15}$$

here, n represents the number of Monte Carlo simulations executed. The standard deviation of the final altitude, velocity, and flight path angle is expressed in Eq. 16:

$$\begin{aligned} \sigma_h^f&=\sqrt{\frac{1}{n}\sum_{i=1}^n (h_i^f-\mu_f)^2} \\ \sigma_v^f&=\sqrt{\frac{1}{n}\sum_{i=1}^n (v_i^f-\mu_f)^2} \\ \sigma_\gamma^f&=\sqrt{\frac{1}{n}\sum_{i=1}^n (\gamma_i^f-\mu_f)^2} \end{aligned} \tag{16}$$

The proposed optimization framework aims to minimize the standard deviation of the final altitude, velocity, and flight path angle, treated as the first, second, and third objectives, respectively. Conversely, maximizing the payload mass is defined as the fourth objective. Consequently, the robust optimization problem is formulated as a weighted-sum multiobjective function, expressed in Eq. 17:

$$\begin{cases} & find \quad x \\ \min & k_1 \dfrac{1}{m_f} + k_2\sigma_h^f + k_3\sigma_v^f + k_4\sigma_\gamma^f \\ & S.t. \quad g(x) \le 0 \\ & \quad\; x^L \le x \le x^U \end{cases} \tag{17}$$

here, the weighting coefficients are assigned as follows: $k_1 = 10^8$, $k_2 = 10^{-3}$, $k_3 = 10^{-1}$, and $k_4 = 10^3$.

It should be emphasized that the selection of weighting coefficients with differing orders of magnitude was primarily aimed at ensuring a balanced contribution of the four performance criteria in the composite objective function. This adjustment was necessitated by the considerable disparities in both scale and magnitude of variation among the parameters—namely, final mass, altitude, velocity, and flight path angle. The weighting factors were determined according to the characteristic output range of each objective function and were empirically tuned to normalize the relative influence of each criterion within the optimization process.

Implementation of robust optimization algorithm

In the problem of optimizing the robust design of the SLV or upper stage, the formulation presented was first used to model the problem. Moreover, to solve the optimization problem, four optimization methods (GA, PSO, GWO, and IWO) were used.

It should also be noted that the parameter values for each optimization algorithm were determined through an iterative trial-and-error process. To ensure reliable performance and adequate convergence behavior, these parameters were carefully tuned during preliminary simulation runs. A summary of the final parameter settings for each algorithm is presented in Table 2.

The complexity of the problem, as well as the Monte Carlo implementation, significantly increased the computational load, so the robust design optimization process required a very long time for continuous execution. The Monte Carlo method required the calculation of the mean and standard deviation of the objective function and the problem constraints. The main effect was an increase in computational load, which slowed down the optimization process (here, the number of Monte Carlo iterations is considered equal to 300). The constraints, along with the mean and standard deviation of the parameters required for implementing the robust design optimization method, are placed in an objective function after normalization using the penalty function method.

SIMULATION RESULTS

In order to show the effect of uncertainties on the SLV trajectory and the performance of optimization methods in the presence of uncertainties, simulation has been implemented in MATLAB-R2020b and tested on a PC with 2.5 GHz Intel Core i5 processor and 16 GB of RAM running the 64-bit Windows 11 operating system.

Additionally, to ensure the reliability of the developed MATLAB-based trajectory simulation code, a validation process was carried out by comparing its outputs to available flight data from real-world launch vehicles. The results demonstrated a high degree of agreement between the simulated trajectories and the actual flight data of the launch vehicles considered.

Table 2. Algorithm parameter tuning.

GA	
Parameter	**Value**
Population Size	100
Elite Count	5
Max Generations	20
Max Stall Generations	5
Function Tolerance	1e-2
Crossover Fcn	@crossoverheuristic
Mutation Fcn	@mutationadaptfeasible
Creation Fcn	@gacreationuniform
PSO	
Parameter	**Value**
Function Tolerance Data	1e-6
Max Iterations Data	100
Min Neighbors Fraction Data	0.25
Self-Adjustment Weight Data	1.49
Social Adjustment Weight Data	1.49
Swarm Size Data	50
GWO	
Parameter	**Value**
Number of Iterations	150
Population Size (Pack Size)	100
IWO	
Parameter	**Value**
Initial Population Size	20
Maximum Population Size	100
Min Seeds Produced	0
Max Seeds Produced	5
Initial Standard Deviation	0.1
Final Standard Deviation	0.001
Number of Iterations	500

Source: Elaborated by the authors.

In the following, the simulation is performed with two approaches: first, the problem is solved by designing a robust optimal trajectory of a two-stage SLV; then, assuming that the design of the first stage of the SLV is already fixed, the trajectory design for the upper stage of this SLV proceeds with this method. For the two approaches, the SLV final desired parameters are considered as follows (Eq. 18):

$$\text{g(x): } [\, h_f = 250Km\,,\; V_f = 7600\frac{m}{s}\,,\; \gamma_f = 0deg\,] \tag{18}$$

First approach (SLV simulation results)

In this approach, for designing a robust optimal trajectory of the SLV, the required parameters are presented in Table 3.

Table 3. The SLV parameters required for simulation.

Parameters	Value
Total weight	102100 (kg)
1st stage thrust	1788000 (N)
2nd stage thrust	157000 (N)
1st stage burning time (t1)	365.4963 (s)
2nd stage burning time (tf)	153.5491 (s)
1st stage specific impulse (Isp1)	291.3 (s)
2nd stage specific impulse (Isp2)	303 (s)
Longitude	–80.54
Latitude	28.5
Initial altitude	0 (km)

Source: Elaborated by the authors.

Additionally, within this framework, the design parameter vector x comprises the initial burning time, the final burning time, and the pitch angle at the first staging, respectively. This vector can be expressed as shown in Eq. 19:

$$x = [t_{b_1}, t_{b_2}, \theta_1] \tag{19}$$

The upper and lower bounds for the decision variable vector in the optimization problem are defined as in Eqs. 20 and 21:

$$x^L = [t_{b_1}^L, t_{b_2}^L, \theta_1^L] = [130, 350, 23]; (\mathrm{Sec}, Deg) \tag{20}$$

$$x^U = [t_{b_1}^U, t_{b_2}^U, \theta_1^U] = [153, 365, 28]; (\mathrm{Sec}, Deg) \tag{21}$$

The simulation of the SLV trajectory's deterministic optimum and robust optimum using four optimization methods—GA, PSO, GWO, and IWO—has been completed. The simulation results have been presented in Table 4.

Table 4. The final SLV parameters in the three modes, the non-optimal, optimal, and the robust optimal.

Parameters	Basic pitch program	Optimal (GA)	Optimal (PSO)	Optimal (GWO)	Optimal (IWO)	Robust Optimal (GA)	Robust Optimal (PSO)	Robust Optimal (GWO)	Robust Optimal (IWO)
1st stage burning Time (t1), sec	134.0711	130.6637	131.6881	130	130.6385	131.0173	131.2	131	130.9361
2nd stage burning Time (tf), sec	358.9201	356.1636	350.1636	360	354.6958	350.9957	350	351.7865	352.724
1st stage pitch angle (θ1), deg	24.65	24.4596	23.8293	24.49	24.5897	23.8408	23.7606	23.7867	23.8321
Final mass (Mass At Seccend Stage Burnout)-(kg)	2920.33	3492.23	3236.18	3228.05	3545.07	3182.8	3115.74	3140.53	3150.29
Run Time (Sec)	-	56.33	101.2	270.1	400.4	1126.7	2726.1	9454.9	11,966.5

Source: Elaborated by the authors.

During the execution of the SLV robust trajectory design simulation, uncertainties can cause differences in parameters, which results in a penalty in the optimization problem. As a result, the amount of propellant the launcher consumes in robust optimization is more significant than in deterministic optimization. Additionally, the first- and second-stage flight times differ in robust optimization. To illustrate this, Fig. 2 shows a comparison of different optimization methods.

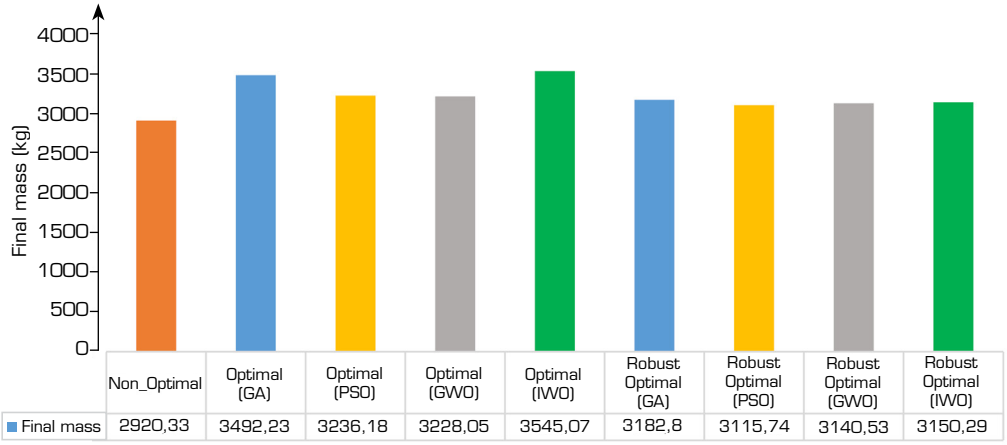

	Non_Optimal	Optimal (GA)	Optimal (PSO)	Optimal (GWO)	Optimal (IWO)	Robust Optimal (GA)	Robust Optimal (PSO)	Robust Optimal (GWO)	Robust Optimal (IWO)
Final mass	2920,33	3492,23	3236,18	3228,05	3545,07	3182,8	3115,74	3140,53	3150,29

Source: Elaborated by the authors.

Figure 2. Comparison of the SLV final mass calculated from the simulation of different optimization methods.

As illustrated in Fig. 3, the simulation results indicate that the SLV successfully achieved the target orbit under both the deterministic optimal and robust optimal approaches, with each method yielding specific final parameter values. Moreover, these images provide a comparison of the flight parameters for the eight optimal and robust optimal design methods.

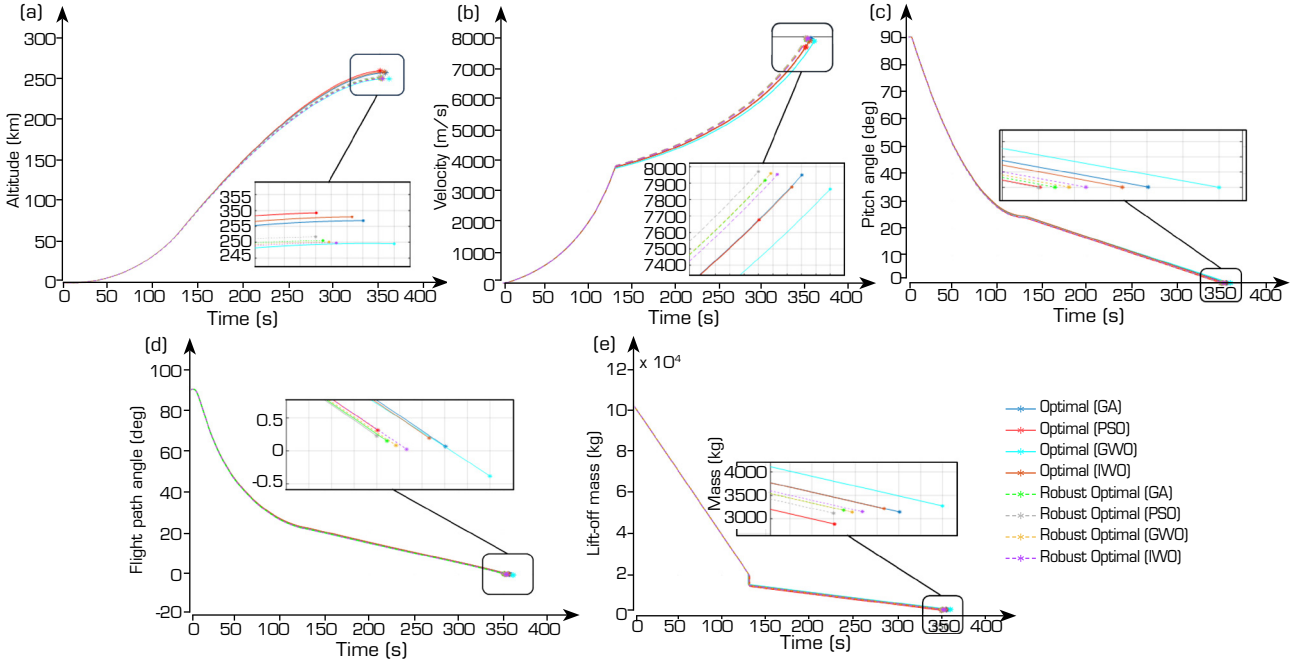

Source: Elaborated by the authors.

Figure 3. comparison of the Satellite Launch Vehicle flight parameters for eight optimal and robust optimal design methods: a) Altitude, b) Velocity, c) Pitch angle(θ), d) Flight Path Angle(γ), e) Lift-off Mass.

To demonstrate the impact of uncertainties listed in Table 1 on an optimal trajectory, a Monte Carlo simulation is used. The results of this simulation are presented in Figures 4 to 6 which show the Altitude, velocity, and Flight Path angle. The final Altitude has a standard deviation of roughly 31 km, indicating that a considerable amount of energy is needed to compensate for this Altitude.

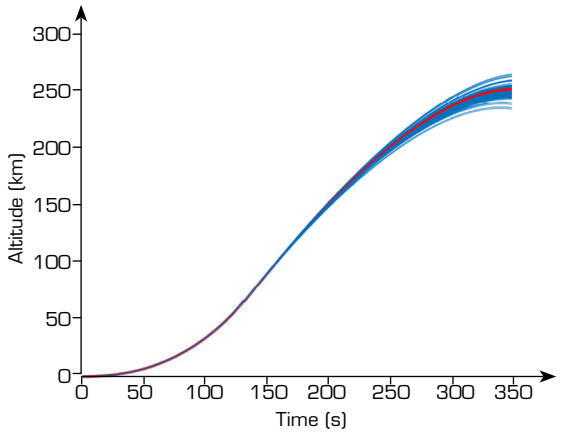

Source: Elaborated by the authors.

Figure 4. The effect of uncertainties on SLV Altitude with deterministic optimal design.

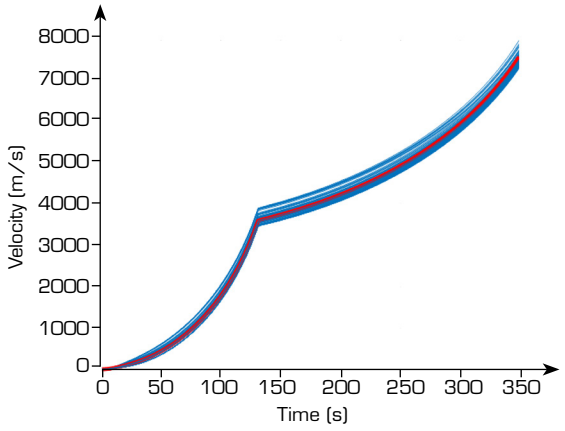

Source: Elaborated by the authors.

Figure 5. The effect of uncertainties on SLV velocity with deterministic optimal design.

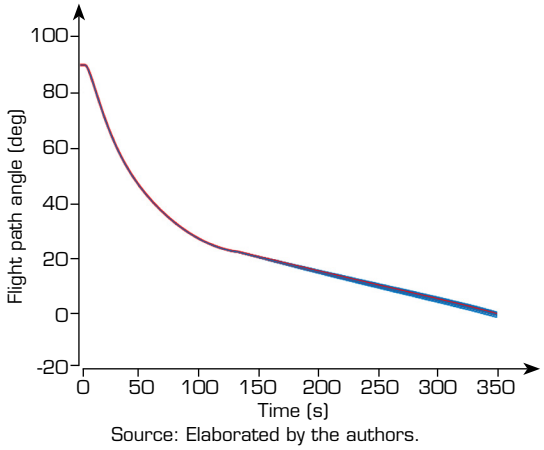

Source: Elaborated by the authors.

Figure 6. The effect of uncertainties on SLV Flight Path angle with deterministic optimal design.

The method of robust optimal design of the SLV trajectory, shown in Fig. 1, was evaluated for the impact of uncertainty using the objective function described in Eq. 14. The uncertainty analysis was performed through Monte Carlo simulation, as explained in Fig. 7 to 9. The standard deviation of the final altitude was found to be approximately 6 km.

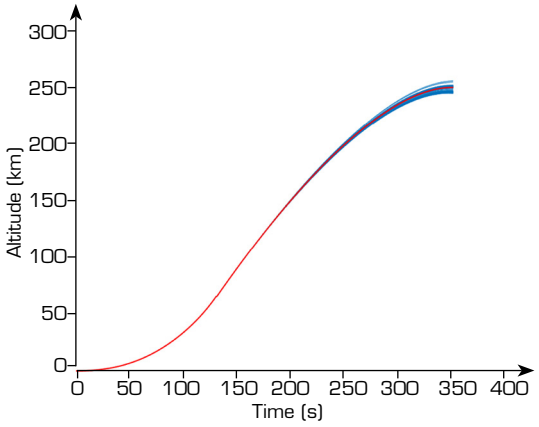

Source: Elaborated by the authors.

Figure 7. Reducing the effect of uncertainties on SLV Altitude with robust optimal design.

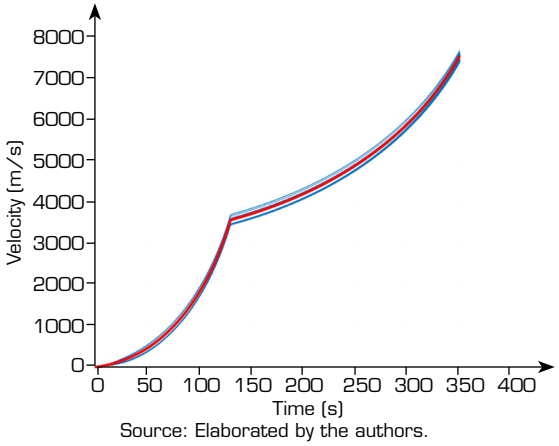

Source: Elaborated by the authors.

Figure 8. Reducing the effect of uncertainties on SLV velocity with robust optimal design.

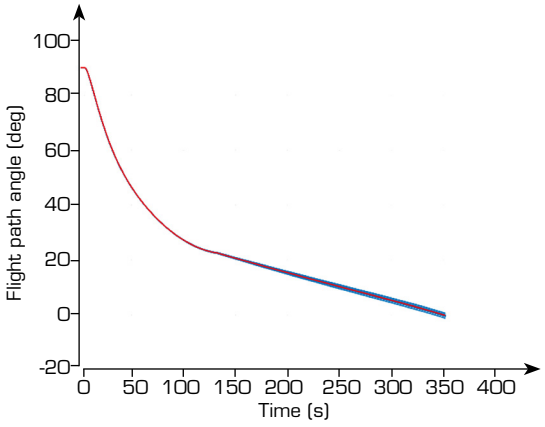

Source: Elaborated by the authors.

Figure 9. Reducing the effect of uncertainties on SLV Flight Path angle with robust optimal design.

Based on Figs. 4 to 9, the impact of the robust optimal design can be observed through the Monte Carlo analysis. This impact is also reflected in Tables 5 and 6, which show the deviation from the standard in the deterministic optimum for the altitude parameter as 31 km, orbital velocity as 950 m·s^{-1}, and flight path angle as 6.7°. However, in the robust optimum, the deviation from the standard for the altitude parameter is only 6 km, the orbital velocity is 100 m·s^{-1}, and the flight path angle is 0.3°.

Table 5. Amount of deviation from the standard in uncertainty analysis for deterministic optimum.

Parameters	$3\sigma_h^{opt}$	$3\sigma_V^{opt}$	$3\sigma_\gamma^{opt}$
Value	31 (km)	950 (m·s^{-1})	6.7 (deg)

Source: Elaborated by the authors.

Table 6. Amount of deviation from the standard in uncertainty analysis for robust optimum.

Parameters	$3\sigma_h^{opt}$	$3\sigma_V^{opt}$	$3\sigma_\gamma^{opt}$
Value	6 (km)	200 (m·s^{-1})	0.3 (deg)

Source: Elaborated by the authors.

Therefore, the robustness of the optimal trajectory has caused the altitude error to be reduced by nearly 25 km and the error in the orbital velocity of 750 m·s^{-1}, as well as this error in the flight path angle to be reduced by 6.4°. Finally, this analysis results demonstrates the positive impact of the robust design algorithm in reducing the final error due to uncertainties.

Second approach (Upper-stage simulation results)

In this approach, for designing a robust optimal trajectory of the upper stage of the mentioned SLV, the required parameters are presented in Table 7.

Table 7. The upper-stage parameters required for simulation.

Parameters	value
Total weight	14900 (kg)
Upper-stage thrust	157000 (N)
Upper-stage burning time (t1)	200 (s)
Upper-stage specific impulse (Isp)	303 (s)
Longitude	55.1873
Latitude	36.2624
Initial altitude	65 (km)

Source: Elaborated by the authors.

Furthermore, in this methodology, the design parameter vector x consists of the upper stage burning time and the pitch angle at the first staging. This vector can be expressed as shown in Eq. 20:

$$x = [t_{b_U}, \theta_1] \tag{20}$$

The upper and lower bounds of the decision variable vector for the optimization problem are defined in Eqs. 21–22:

$$x^L = [t_f^L, \theta_f^L] = [100, 15]; (\text{Sec}, Deg) \tag{21}$$

$$x^U = [t_f^U, \theta_f^U] = [250, 30]; (\text{Sec}, Deg) \tag{22}$$

After simulating the deterministic optimum and the robust optimum of the upper-stage trajectory with four optimization methods, GA, PSO, GWO, and IWO, the results of the simulation are presented in Table 8.

Table 8. The final upper-stage parameters in the three modes: the non-optimal, optimal, and the robust optimal.

Parameters	Basic pitch program	Optimal (GA)	Optimal (PSO)	Optimal (GWO)	Optimal (IWO)	Robust Optimal (GA)	Robust Optimal (PSO)	Robust Optimal (GWO)	Robust Optimal (IWO)
Upper-stage burning time (t_f), s	226.8491	219.9245	220	220.591	221.9869	221.9891	221.64	223.880	224.193
Stage pitch angle (θ_1), deg	22.05	22.5001	21.4	21.3222	21.1463	21.15	21.22	21.0076	20.861
Final mass (mass at end of burning)-(kg)	2951.16	3215.34	3268.18	3268.18	3215.34	3109.67	3162.51	3114.32	3098.47
Propellant consumption	11948.84	11684.66	11631.82	11631.82	11684.66	11790.33	11737.49	11785.6	11801.5
Run time (s)	-	8	9.2	18.8	60	268.2	447.8	1894.7	4796.4

Source: Elaborated by the authors.

By executing robust design simulation in the presence of uncertainties, the differences in parameters due to uncertainty cause a penalty in the optimization problem in such a way that the amount of propellant consumed by the launcher in robust optimization is more significant than the deterministic optimum, and the flight time also increases in robust optimization. This comparison and the result of different optimization methods are shown in Fig. 10.

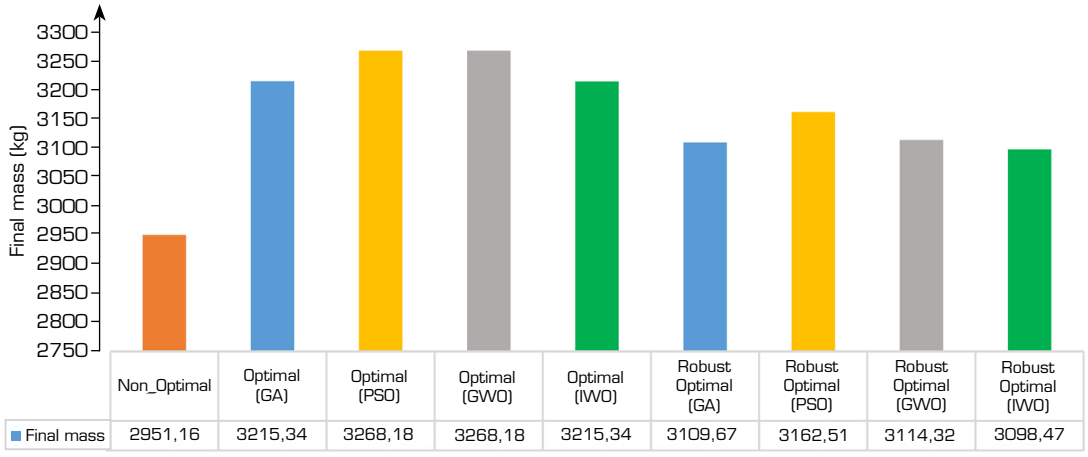

Source: Elaborated by the authors.

Figure 10. Comparison of the upper-stage final mass calculated from the simulation of different optimization methods.

According to the simulation results, Fig. 11 demonstrates that the upper stage of the launcher successfully reached the target orbit in both the deterministic optimal and robust optimal approaches, with distinct final parameter values observed in each case. The figure also shows the comparison of flight parameters for two deterministic and robust optimal approaches.

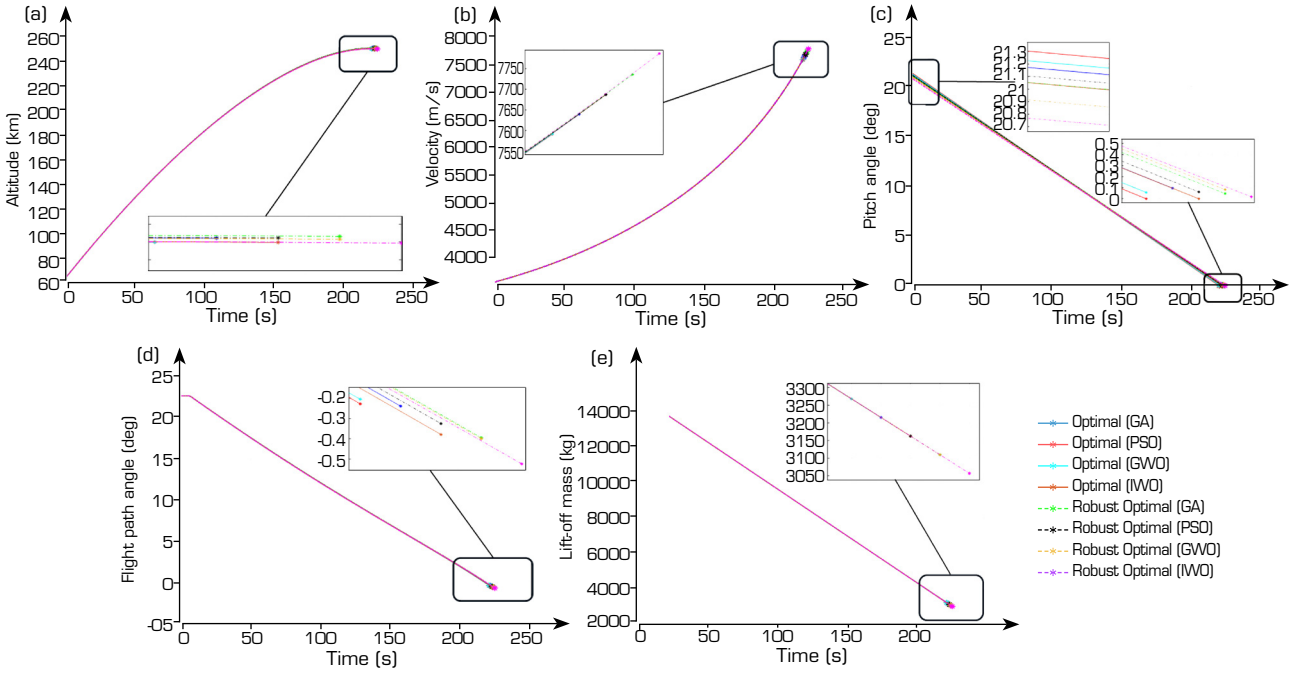

Source: Elaborated by the authors.

Figure 11. Comparison of the upper-stage flight parameters for eight optimal and robust optimal design methods: A) Altitude, B) Velocity, C) Pitch angle(θ), D) Flight Path Angle(γ), E) Lift-off Mass.

A Monte Carlo simulation is used to demonstrate the impact of uncertainties on an optimal trajectory (Table 1). The results are analyzed and presented in Figs. 12–14, which show the altitude, velocity, and flight path angle. The final altitude has a standard deviation of approximately 22 km, meaning that a significant amount of energy is required to compensate for this orbital altitude.

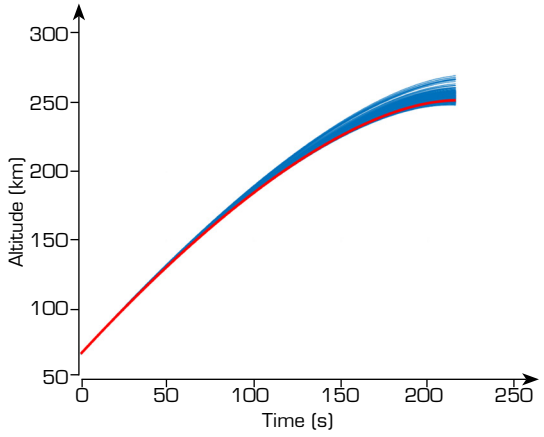

Source: Elaborated by the authors.

Figure 12. The effect of uncertainties on upper-stage altitude with deterministic optimal design.

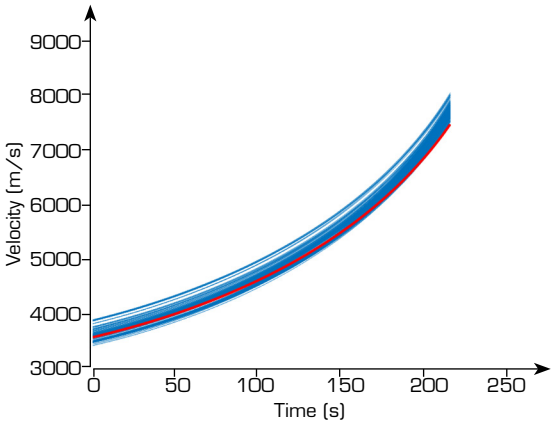

Source: Elaborated by the authors.

Figure 13. The effect of uncertainties on upper-stage velocity with deterministic optimal design.

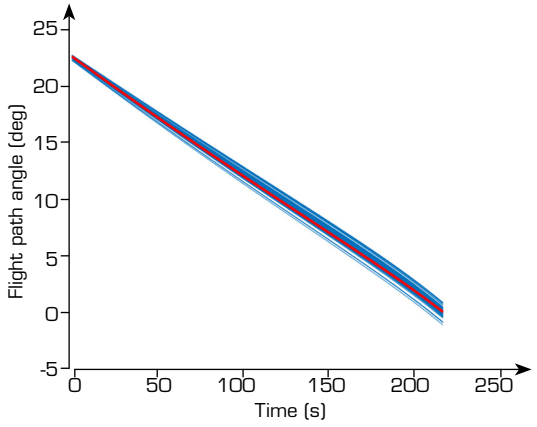

Source: Elaborated by the authors.

Figure 14. The effect of uncertainties on upper-stage flight path angle with deterministic optimal design.

Due to applying the robust optimal design of the upper-stage trajectory, as depicted in Fig. 1, the impact of uncertainty on the design was evaluated using the objective function outlined in Eq. 14. The uncertainty analysis was carried out using Monte Carlo simulation, as detailed in Figs. 15–17. The standard deviation of the final Altitude was determined to be approximately 5 km.

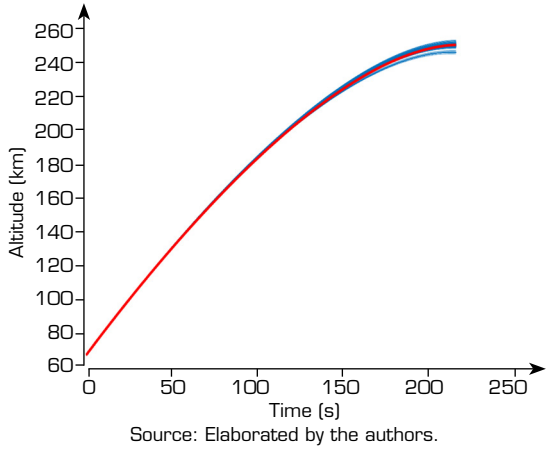

Source: Elaborated by the authors.

Figure 15. Reducing the effect of uncertainties on upper-stage altitude with robust optimal design.

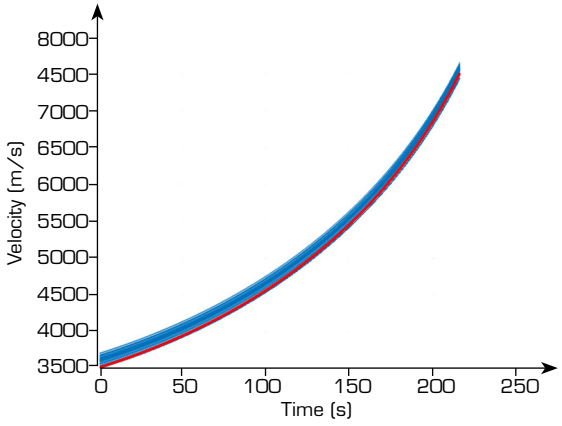

Source: Elaborated by the authors.

Figure 16. Reducing the effect of uncertainties on upper-stage velocity with robust optimal design.

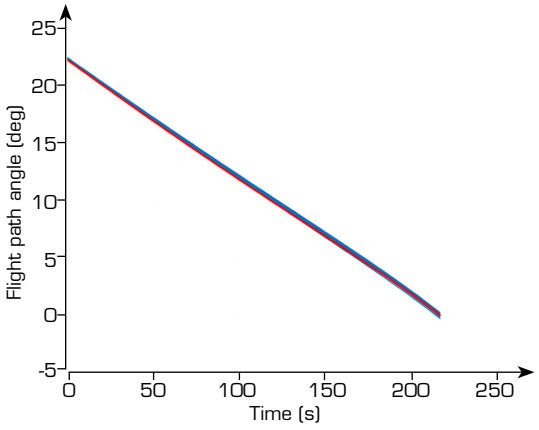

Source: Elaborated by the authors.

Figure 17. Reducing the effect of uncertainties on upper-stage flight path angle with robust optimal design.

Based on Figs. 12–17, the impact of the robust optimal design can be observed through the Monte Carlo analysis. This impact is also reflected in Tables 9 and 10, which show the deviation from the standard in a deterministic optimum for the altitude parameter as 22 km, orbital velocity as 800 m·s^{-1}, and flight path angle as 2.03°. However, in the robust optimum, the deviation from the standard for the altitude parameter is only 5 km, orbital velocity is 150 m·s^{-1}, and flight path angle is 0.17°.

Table 9. Amount of deviation from the standard in uncertainty analysis for deterministic optimum.

Parameters	$3\sigma_h^{opt}$	$3\sigma_V^{opt}$	$3\sigma_\gamma^{opt}$
Value	22 (km)	800 (m·s^{-1})	2.03 (deg)

Source: Elaborated by the authors.

Table 10. Amount of deviation from the standard in uncertainty analysis for Robust optimum.

Parameters	$3\sigma_h^{opt}$	$3\sigma_V^{opt}$	$3\sigma_\gamma^{opt}$
value	5 (km)	150 (m·s^{-1})	0.17 (deg)

Source: Elaborated by the authors.

Therefore, the robustness of the optimal trajectory has caused the altitude error to be reduced by nearly 17 km and the error in the orbital velocity of 650 $m \cdot s^{-1}$, as well as this error in the flight path angle to be reduced by 1.86°. Ultimately, the analysis results can demonstrate the efficiency of the robust design algorithm's performance.

CONCLUSION

In practical flight scenarios, the performance of a SLV often deviates from deterministic simulation results due to inherent design uncertainties and external disturbances encountered during the ascent phase. To improve mission success rates, it is essential to account for these uncertainties during the design phase. A critical element of this approach is the development of a robust trajectory, which mitigates control system complexity and reduces the operational load on actuators. By addressing these factors systematically, the overall reliability and efficiency of the mission can be substantially enhanced.

This study evaluates four metaheuristic robust optimization algorithms—GA, PSO, GWO, and IWO—to optimize the pitch program, aiming to enhance the robustness of the SLV and its upper stage against existing uncertainties.

It is crucial to identify an optimal trajectory that is robust against uncertainties. This leads to better flight performance, reduced steering-control system workload, and increased SLV reliability.

To achieve the objective, a comprehensive analysis was conducted to design an effective and efficient trajectory for a two-stage SLV. This entailed developing an optimal trajectory for both stages of the SLV. Then, the upper stage trajectory was designed assuming that the trajectory for the SLV's first stage had already been fixed and could not be changed. The goal was to ensure that the final trajectory of the SLV and upper stage was robust, safe, and optimized for maximum payload mass, with three-dimensional equations of motion as constraint equations.

Based on the simulation results, it is evident that the first approach is more efficient. This is because the trajectory of the first stage of the SLV can be designed and adjusted, enabling better optimization. The percentage of improvement in the robust optimization methods is higher in the first approach.

According to the first approach, the IWO algorithm delivered the best deterministic performance, achieving the highest payload of 3545.8 kg, while the GA provided the most robust optimization outcome with a payload of 3182.8 kg. In the second approach, the deterministic optimization yielded the best results using PSO and GWO, both attaining payloads of 3268.9 kg, whereas for robust optimization, PSO achieved the most efficient result with a payload of 3162.5 kg.

A deeper evaluation of algorithmic complexity, convergence behavior, and scalability shows that PSO achieved the fastest convergence and lowest computational cost (≈ 100 s for the full SLV and ≈ 9 s for the upper-stage deterministic run); GA exhibited moderately fast but stable convergence (≈ 56 and 8 s for deterministic cases, respectively), maintaining consistency in both deterministic and robust modes; GWO demonstrated balanced but slower convergence (≈ 270 s and 19 s for deterministic runs), while IWO required the highest computational effort due to its iterative seed propagation process (≈ 400 s and 60 s for deterministic runs). Under robust conditions, the computational load increased significantly; GA and PSO reached acceptable results after < 3,000 s, whereas GWO and IWO required > 9,000 s and > 11,000 s respectively.

Overall, GA achieved the best trade-off between robustness and precision, maintaining smaller deviations in altitude and orbital velocity under uncertainty, while PSO delivered superior speed and computational efficiency, suitable for preliminary trajectory design. GWO proved algorithmically scalable and accurate but slower, and IWO, though the most thorough, exhibited the highest complexity and least scalability. These findings validate that convergence speed and robustness are inversely correlated: algorithms with greater population diversity (like GA) ensure higher stability against uncertainty at the cost of execution time, whereas swarm-based methods (like PSO) yield faster solutions but are more sensitive to local minima.

The optimizer model was subjected to Monte Carlo simulation for 300 iterations to account for uncertainties and improve the optimization process. The simulation results showed that the robust optimal trajectory improved the altitude error of the upper stage by nearly 77%, the orbital velocity error by 68%, and the flight path angle error by nearly 90%. Similarly, for the SLV, the robust optimal trajectory improved the altitude error by nearly 80%, the orbital velocity error by 78%, and the flight path angle error by nearly 95% in the presence of uncertainties. Based on the simulation results, it can be concluded that the claim is valid.

Considering the simulation execution time and based on Tables 4 and 8, it should be acknowledged that the results are similar across almost all methods. However, some of the methods used in this study reach the solution in significantly shorter times compared to others.

Finally, it is suggested that GA and PSO methods be used in research because they provide acceptable answers and the time to reach the answer.

CONFLICT OF INTEREST

No conflict of interest.

AUTHORS' CONTRIBUTION

Conceptualization: Arani SAS and Nosratollahi M; **Methodology:** Arani SAS, Nosratollahi M and Abbasi Y; **Software:** Arani SAS; **Analysis:** Arani SAS and Nosratollahi M; **Writing – Original Draft:** Arani SAS, Nosratollahi M and Adami AH; **Writing – Review and Editing:** Arani SAS, Nosratollahi M and Adami AH; **Investigation:** Arani SAS and Nosratollahi M; **Data Curation:** Arani SAS and Nosratollahi M; **Supervision:** Arani SAS and Nosratollahi M; **Final approval:** Nosratollahi M.

DATA AVAILABILITY STATEMENT

All data sets were generated or analyzed in the current study.

FUNDING

Not applicable.

DECLARATION OF USE OF ARTIFICIAL INTELLIGENCE TOOLS

The authors confirm that software (Grammarly) was used only for language polishing and grammar correction. No AI tools were used for data analysis, algorithm development, simulations, results generation, or interpretation.

ACKNOWLEDGMENTS

Not applicable.

REFERENCES

Abdelhamid AA, El-Kenawy ESM, Ibrahim A, Eid MM, Khafaga DS, Alhussan AA, Mirjalili S, Khodadadi N, LimWH, Shams MY (2023) Innovative feature selection method based on hybrid sine cosine and dipper throated optimization algorithms. IEEE Access 11: 79750-79776. https://doi.org/10.1109/ACCESS.2023.3298955

Adami A, Mortazavi M, Nosratollahi M (2017) A new approach to multidisciplinary design optimization of solid propulsion system including heat transfer and ablative cooling. J Aerosp Technol Manag 9(1):71-82. https://doi.org/10.5028/jatm.v9i1.717

Ansaripour MR, Karimi J, Jamilnia R, Adami A (2019) Designing the optimal ascending Trajectory of the launch Vehicle using the direct launch method. Paper presented at 6th National Conference on Applied Research in Electrical, Mechanical and Mechatronic Engineering, Tehran. In Persian. https://civilica.com/doc/1129939/

Bataleblu AA, Roshanian J, Ebrahimi M (2011) Robust Design Optimization of a Launch Vehicle with Liquid propellant (master's thesis). Tehran.

El-Kenawy ESM, Ibrahim A, Mirjalili S, Zhang YD, Elnazer S, Zaki RM (2022) Optimized ensemble algorithm for predicting metamaterial antenna parameters. Comput Mater Con 71(2):4989-5003. https://doi.org/10.32604/cmc.2022.023884

El-Kenawy ESM, Khodadadi N, Mirjalili S, Abdelhamid AA, Eid MM, Ibrahim A (2024) Greylag goose optimization: Nature-inspired optimization algorithm. Expert Syst Appl 238(E):122147. https://doi.org/10.1016/j.eswa.2023.122147

Ghapanvary MA, Nosratollahi M, Karimi J (2021) Dynamic response analysis of a high glide ratio parachute system. Int J Eng 34(1):195-201. https://doi.org/10.5829/IJE.2021.34.01A.22

Grant MJ, Bolender MA (2016) Rapid, robust trajectory design using indirect optimization methods. Paper presented at AIAA Atmospheric Flight Mechanics Conference. Elsevier; Dallas, USA. https://doi.org/10.2514/6.2015-2401

Haimes YY, Barry T, Lambert JH (1994) When and how can you specify a probability distribution when you don't know much? Risk Anal 14(5):661-706. https://doi.org/10.1111/j.1539-6924.1994.tb00280.x

Hattis D, Burmaster DE (1994) Assessment of variability and uncertainty distributions for practical risk analyses. Risk Anal 14(5):713-730. https://doi.org/10.1111/j.1539-6924.1994.tb00282.x

Hosseini M, Toloie A, Nosratollahi M, Adami A (2011) Multidisciplinary design optimization of an expendable launch vehicle. Paper presented at Proceedings of 5th International Conference on Recent Advances in Space Technologies-RAST2011, 702-707. IEEE.

Karim FK, Khafaga DS, Eid MM, Towfek SK, Alkahtani HK (2023) A novel bio-inspired optimization algorithm design for wind power engineering applications time-series forecasting. Biomimetics 8(3):321. https://doi.org/10.3390/biomimetics8030321

Khodadadi N, Khodadadi E, Al-Tashi Q, El-Kenawy ESM, Abualigah L, Abdulkadir SJ (2023) BAOA: Binary Arithmetic Optimization Algorithm with K-Nearest Neighbor Classifier for Feature Selection. IEEE Access 11:94094-94115. https://doi.org/10.1109/ACCESS.2023.3310429

Liu X, Lu P (2013) Robust Trajectory Optimization for Highly Constrained Rendezvous and Proximity Operations. Paper presented at AIAA Guidance, Navigation, and Control (GNC) Conference. AIAA; Boston, USA. https://doi.org/10.2514/6.2013-4720

Luo YZ, Yang Z (2017) A review of uncertainty propagation in orbital mechanics. Prog Aerosp Sci 89:23-39. https://doi.org/10.1016/j.paerosci.2016.12.002

Mehrabian AR, Lucas C (2006) A novel numerical optimization algorithm inspired from weed colonization. Ecol Inform 1(4):355-366. https://doi.org/10.1016/j.ecoinf.2006.07.003

Mirjalili S, Mirjalili SM, Lewis A (2014) Grey Wolf Optimizer. Adv Eng Softw 69:46-61. https://doi.org/10.1016/j.advengsoft.2013.12.007

Mirshams M, Roshanian J, Dehkordi SY, Bataleblu AA (2016) Launch vehicle collaborative robust optimal design with multiobjective aspect and uncertainties. J Modares Mech Eng 15(11):339-350. https://mme.modares.ac.ir/article_8872_en.html

Niazi S, Toloei A, Ghasemi R (2024) Improving performance of flight control system in presence of uncertainties and extreme changes in parameters using multiple model adaptive control. Int J Eng Trans A Basics 37(10):2030-2041. https://www.ije.ir/article_192332.html

Okada M, Pekarovskiy A, Buss M (2015) Robust trajectory design for object throwing based on sensitivity for model uncertainties. Paper presented at IEEE International Conference on Robotics and Automation. IEEE; Seattle, USA. https://doi.org/10.1109/ICRA.2015.7139623

Padmanabhan D (2003) Reliability-based optimization for multidisciplinary system design (doctoral dissertation). Indiana: University of Notre Dame.

Paiva RM, Crawford C, Suleman A (2014) Robust and reliability-based design optimization framework for wing design. AIAA J 52(4):711-724. https://doi.org/10.2514/1.J052161

Roshanian J, Bataleblu AA, Ebrahimi M (2011) Robust Design Optimization of a Launch Vehicle with Liquid propellant. (MSc Thesis). Tehran. In Persian. https://elmnet.ir/doc/10570577-71331

Rostami RH, Toloei A (2015) Mid-course trajectory design of a ground-to-air missile using GA and PSO (MS.c Thesis). Tehran. In Persian.

Selim A, Ozkol I (2023) Multi-phase robust optimization of a hybrid guidance architecture for launch vehicles. Paper presented at 10th European Conference for Aeronautics And Space Sciences. EUCASS; Lausanne, Switzerland. https://doi.org/10.13009/EUCASS2023-396

Sentz K, Ferson S (2002) Combination of evidence in Dempster-Shafer theory. SAND2002-0835, Sandia National Laboratories.

Shaver A, Hull DG (1990) Advanced launch system trajectory optimization using suboptimal control. Paper presented at AIAA GNC Conference.

Shi Y, Lan Q, Lan X, Wu J, Yang T, Wang B (2023) Robust optimization design of a flying wing using adjoint and uncertainty-based aerodynamic optimization approach. Struct Multidisc Optim 66:110. https://doi.org/10.1007/s00158-023-03559-z

Su Z, Wang H (2015) A novel robust hybrid gravitational search algorithm for reusable launch vehicle approach and landing trajectory optimization. Neurocomp 162:116-127. http://doi.org/10.1016/j.neucom.2015.03.063

Taheri MR, Soleymani A, Toloei A, Vali AR (2013) Performance evaluation of the high-altitude launch technique to orbit using atmospheric properties. Int J Eng 26(4):333-340.

Talouki IF, Toloei A (2025) Optimization of flight endurance for turboprop air taxis using metaheuristic algorithms. Int J Eng Trans A Basics 38(7):1685-1698. https://doi.org/10.5829/ije.2025.38.07a.19

Vinh N (1981) Optimal Trajectories in Atmospheric Flight. New York: Elsevier.

Wazed MA, Ahmed S, Yusoff N (2009) Uncertainty factors in real manufacturing environment. Aust J Basic Appl Sci 3(2): 342-351. https://ajbasweb.com/old/ajbas/2009/342-351.pdf

Xue Q, Duan H (2017) Robust attitude control for reusable launch vehicles based on fractional calculus and pigeon-inspired optimization. IEEE/CAA J Autom Sinica 4(1):89-97. https://doi.org/10.1109/JAS.2017.7510334

Yager R, Kacprzy KJ, Fedrizzi M (1994) Advances in the Dempster-Shafer theory of evidence. New York: John Wiley and Sons.

Yao W, Chen X, Luo W, van Tooren M, Guo J (2011) Review of uncertainty-based multidisciplinary design optimization methods for aerospace vehicles. Prog Aerosp Sci 47(6):450-479. https://doi.org/10.1016/j.paerosci.2011.05.001

Youn BD, Wang P (2006) Bayesian reliability-based design optimization under both aleatory and epistemic uncertainties. Paper presented at 11th AIAA/ISSMO Multidisciplinary Analysis and Optimization Conference, Portsmouth, Virginia; A1AA-2006-692S. https://doi.org/10.2514/6.2006-6928

Zardashti R, Jafari M, Hosseini SM, Arani SAS (2020) Robust optimum trajectory design of a satellite launch vehicle in the presence of uncertainties. J Aerosp Tecnol Manag 12:e3520. https://doi.org/10.5028/jatm.v12.1176

Zhao J, Hu H, Han Y, Cai Y (2023) A review of unmanned vehicle distribution optimization models and algorithms. J Traffic Transp Eng 10(4):548-559. https://doi.org/10.1016/j.jtte.2023.07.002

Zheng Y, Fu X, Xu M, Li Q, Lin M (2020) Ascent trajectory design of small-lift launch vehicle using hierarchical optimization. Aerosp Sci Technol 107:106285. https://doi.org/10.1016/j.ast.2020.106285

Zipfel PH (2007) Modeling and Simulation of Aerospace Vehicle Dynamics-American Institute of Aeronautics and Astronautics. AIAA Education Series.